# Memory Effects in Supramolecular Networks of Diacids and Polyfunctional Pyridine Derivatives

**Kurt N. Wiegel,[1] Anselm C. Griffin,[2] Micah S. Black,[3] David A. Schiraldi[4]**

[1]*Department of Chemistry, University of Wisconsin-Eau Claire, Eau Claire, Wisconsin 54702*
[2]*School of Polymer, Textile, and Fiber Engineering, Georgia Institute of Technology, Atlanta, Georgia 30332*
[3]*School of Polymers and High-Performance Materials, The University of Southern Mississippi, Hattiesburg, Mississippi 39406*
[4]*Department of Macromolecular Science and Engineering, Case Western Reserve University, Cleveland Ohio 44106-7202*

Received 2 October 2003; accepted 19 December 2003

**Abstract:** Highly crosslinked networks were produced through a series of diacids and tetrakis pyridyls. These materials displayed complex crystallization behaviors over multiple heat/cool cycles. The shifting of crystallization behaviors with time in the melt phase seems to indicate that the materials move toward thermodynamically ideal structures. This behavior is suggestive of a type of memory in which the networks remember the morphological structure previous to the melt and improve upon that structure in the next cooling cycle. The network/memory phenomena observed in small molecule diacid/tetrapyridyl systems also appeared to exist when poly(ethylene terephthalate) (PET) polymer was used as the source of carboxylic acid functionalities. The same time- dependent behaviors, suggestive of sequential steps toward thermodynamically optimum states, were observed when the PET/tetrapyridyl systems were thermally cycled. It was also observed that complexation of tetrapyridyl with PET brought about a significant change in oxygen gas barrier properties; these changes were opposite to those obtained when covalent crosslinks were introduced into PET. © 2004 Wiley Periodicals, Inc. J Appl Polym Sci 92: 3097–3106, 2004

**Key words:** supramolecular; hydrogen bonding; networks; crystallization; transport; polyesters

## INTRODUCTION

The use of hydrogen bonds as a means of achieving supramolecular assembly in man-made oligomers and polymers is an area of great scientific interest. The design of such hydrogen-bonded systems as a means of tuning in properties was explored as a means of producing durable, smart materials.[1] Static structures produced in this manner range from nanotubes[2] and enzyme-like systems[3] to the early forms of molecular machines.[4] Hydrogen bonding was used to modify preexisting polymer chains[5] or to associate different main-chains with one another. The later approach exploits the labile nature of hydrogen bonds to produce dynamic chain lengths.[6] A living polymer system can be produced in which the chain configuration is capable of reorganization, macroscale rearrangement (of morphology and structure), annealing, healing, and possibly other adaptation processes dependent on thermal or solvent treatment.[7] Early work in this field showed the formation of molecular and polymeric aggregates through the formation of main- and side-chain hydrogen bonds.[8–22] The formation of networks by using hydrogen bonds has been a more recent area of study; these networks were formed through the association of side-chain interactions on a preexisting polymer chain or through the association of the hydrogen bonds throughout the network. Meijer and coworkers have investigated the application of a quadruple-hydrogen-bond associative structure to form supramolecular networks that were found to be mechanically more stable than their covalent analogs.[23] Previous work undertaken in our laboratory[24] includes the use of a single tetrafunctional netpoint to create a supramolecular network. These materials were synthesized in an effort to overcome the thermal lability of the single- associative chain structures while still maintaining a dynamic molecular weight. The networks produced in this manner were found to form fibers and display glass transitions and cold crystallization.

The focus of the current work is on the synthesis of a series of multifunctional pyridyl netpoints. These netpoints are used to form three-dimensional supramolecular network complexes with a well-studied diacid.[23] The networks are then characterized to determine the influence of hydrogen bond connectivity on their thermal properties and to probe the effect of reversibility of network structure in a supramolecular species. Additionally, the effect of a tetrafunctional pyridyl additive upon thermal and transport behav-

*Correspondence to:* K. N. Wiegel (WIEGELKN@uwec.edu).
Contract grant sponsor: KoSa.
Contract grant sponsor: NSF-EPSC.R.

Journal of Applied Polymer Science, Vol. 92, 3097–3106 (2004)

iors of poly(ethylene terephthalate) (PET) will be examined, as a probe of supramolecular structure.

## EXPERIMENTAL

### Analysis

All networks formed were analyzed by a TA Instruments DSC 2920 differential scanning calorimeter in hermetically sealed aluminum pans. Heating rates were 10°C/min. Wide-angle X-ray diffraction data were obtained by using a Siemens XPD-700P polymer diffraction system with a two-dimensional, position-sensitive detector.

### Synthesis

All reagents listed were purchased from Aldrich Chemical Co. (Milwaukee, WI) and used as received unless otherwise stated. The syntheses of tetrakis(4-pyridyloxymethylene)methane, tetrakis(tosylmethylene)methane, and tetraethyleneglycoxy bis-4-benzoic acid have been reported previously.[24]

#### Tetrakis(3-pyridyloxymethylene)methane

3-Hydroxy pyridine (58.6 g, 617.4 mmol), tetrakis (tosylmethylene) methane (116.07 g, 154.3 mmol), cesium carbonate (201 g, 617.4 mmol), and 150 mL DMF were combined in a 2-L three-necked round-bottom flask and fitted with an overhead mechanical stirrer with a poly(tetrafluorethylene)(PTFE) paddle. The mixture was refluxed for 24 h with stirring. The mixture was then poured into two 4-L portions of water and refrigerated for 12 h. The tan precipitate was isolated by filtration under vacuum and recrystallized (MeOH/$H_2O$) to provide 68.5 g of product.

Yield: 78.7%). Melting point (150°C. IR (KBr, $cm^{-1}$): 3067, 2941, 2345, 1575, 1475, 1431, 1271, 1232, 1055, 802. $^1$H-NMR ($CDCl_3$, ppm.): 8.24 (4H, m, pyridyl), 8.22 (4H, m, pyridyl), 7.23 (8H, m, pyridyl), 4.41 (8H, s, methylene). $^{13}$C-NMR ($CDCl_3$, ppm): 142.8, 140.3, 138.0, 123.9, 121.25, 66.4, 45.1.

#### Triethyleneglycoxy bis-4-benzoic acid

Triethyleneglycol bis(*p*-tosylate) (10 g, 21.8 mmol), ethyl *p*-hydroxybenzoate (7.25 g, 43.6 mmol), cesium carbonate (14.26 g, 43.6 mmol), and 150 mL acetone were combined in a 250-mL one-necked round-bottom flask. The mixture was refluxed with stirring for 48 h under an argon atmosphere. A white precipitate was isolated by filtration under vacuum and washed with three 100-mL fractions of acetone. Excess solvent was removed from the filtrate under reduced pressure and an oil was collected. The oil was dissolved in 150 mL of ethanol; then, to this solution, 150 mL of aqueous 10% NaOH solution was added. This mixture was refluxed for 2 h, after which the ethanol was removed from the mixture under reduced pressure, and the resulting solution was strongly acidified with concentrated HCl. A white precipitate was isolated by vacuum filtration. This solid was air dried and recrystallized (EtOH) to provide 7.32 g of white powder.

Yield: 73.2%. mp: 237.1°C. IR: (KBr, $cm^{-1}$). Broad OH centered at 3000, 2874, 1678, 1602, 1431, 1300, 1263, 1170, 1132. $^1$H-NMR (DMSO-$d_6$, ppm): 7.824 (4H, d, phenyl), 7.03 (4H, d, phenyl), 4.04 (4H, d, phenyl), 4.17 (4H, t, Ph—O—C$H_2$—), 3.77 (4H, t, Ph—O—$CH_2$—C$H_2$—) 3.63 (4H, s, Ph—O—$CH_2$—$CH_2$—O—C$H_2$—). $^{13}$C-NMR (DMSO-$d_6$, ppm): 167.98 (Carbonyl), 162.11, 131.36, 123.02, 114.30, 69.9, 68.8, 67.4.

#### Pentaethyleneglycoxy-bis-4-benzoic acid

Pentaethyleneglycol bis(*p*-tosylate) (10 g, 18.3 mmol), ethyl-*p*-hydroxybenzoate (7.25 g, 36.6 mmol), cesium carbonate (11.96 g, 36.6 mmol), and 150 mL of acetone were combined in a 250-mL one-necked round-bottom flask. The mixture was refluxed with stirring for 48 h under an argon atmosphere. The white precipitate formed was isolated by filtration under vacuum and washed with three 100-mL fractions of acetone. Excess solvent was removed from the filtrate under reduced pressure and an oil was collected. This oil was dissolved in 150 mL of ethanol. To this solution, 150 mL of aqueous 10% NaOH solution was added. This mixture was refluxed for 2 h, after which the ethanol was removed from the mixture under reduced pressure, and the resulting solution was strongly acidified with concentrated HCl. A white precipitate was isolated by vacuum filtration; this solid was air dried and recrystallized (EtOH) to provide 4.15 g of white powder.

Yield: 47.7%, mp: 174°C IR (KBr, $cm^{-1}$): 3000, 2880, 2666, 1682, 1605, 1578, 1430. $^1$H-NMR (DMSO-$d_6$, ppm): 12.63 (2H, s, acid) 7.87 (4H, d, phenyl), 7.01 (4H, d, phenyl), 4.14 (4H, t, Ph—O—C$H_2$—), 3.78 (4H, t, Ph—O—$CH_2$—C$H_2$—), 3.36–3.68 (12H, m, ethylene). $^{13}$C-NMR (DMSO-$d_6$, ppm): 167.9, 163.0, 132.2, 123.9, 115.1, 70.8, 70.7, 69.6, 68.3. Elemental anal. calcd for $C_{24}H_{30}O_{10}$: C, 60.24; H, 6.32; Found: C, 60.10; H, 6.30.

#### Tetraethyleneglycoxy-bis(3-methoxy-4-benzoic acid)

Methyl vanillate (5 g, 27.4 mmol) was added to 150 mL of acetone in a 250-mL one-necked round-bottomed flask. Tetraethyleneglycol bis(*p*-tosylate) (6.889 g, 13.72 mmol) and cesium carbonate (8.96 g, 27.4 mmol) were then added, and the mixture was refluxed for 24 h under an argon atmosphere. The white precipitate was isolated by filtration under vacuum and washed with three 100-mL fractions of acetone. Excess solvent was removed from the filtrate under reduced pressure and an oil was collected. The oil was dissolved in 150 mL of ethanol; then, to this solution 150 mL of aqueous 10% NaOH solution was added. The

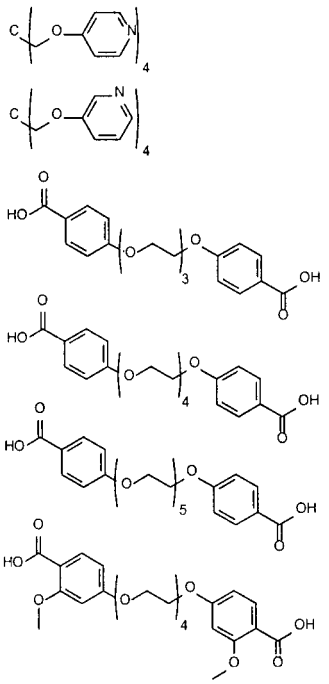

Tetrakis(4-pyridyloxymethylene)methane p

Tetrakis(3-pyridyloxymethylene)methane m

Triethyleneglycoxy bis-4-benzoic acid 3

Tetraethyleneglycoxy bis-4-benzoic acid 4

Pentaethyleneglycoxy bis-4-benzoic acid 5

Tetraethyleneglycoxy bis-(3-methoxy-4-benzoic acid) 4s

**Figure 1** Materials and abbreviations.

mixture was refluxed for 2 h, after which the ethanol was removed from the mixture under reduced pressure, and the resulting solution strongly acidified with concentrated HCl. A white precipitate was isolated by vacuum filtration. This solid was air dried and recrystallized (EtOH) to provide 4.4 g of a white powdery solid.

Yield: 65%. mp: 154EC I.R. (KBr, $cm^{-1}$): 3000, 2775, 1685, 1601, 1425, 1275, 1138. $^1H$—NMR (DMSO-$d_6$, ppm): 7.02 (2H, s, aromatic), 6.99 (2H, d, aromatic), 6.97 (2H, d, aromatic), 4.15 (4H, t, Ar—O—$CH_2$—$CH_2$), 3.81 (6H, s, $CH_3$—O— Ar), 3.77 (4H, t, Ar—O—$CH_2$—$CH_2$—), 3.52–3.57 (12H, m, interior ethylenes). $^{13}C$—NMR (DMSO—$d_6$, ppm): 167.1, 151.9, 148.4, 123.0 (3 carbons), 69.9, 69.8, 68.7, 67.9, 55.4.

## Network formation

All networks were formed on the basis of the following procedure. A stoichiometric mixture of the hydrogen-bond donors (bisacids) and acceptors (tetrakispyridyls) were combined. A balance was maintained at all times between acid protons and pyridyl nitrogens. The mixture was placed into a 5 mL microscale conical vial, sealed with a PTFE cap, and flushed with argon. The vial was then lowered into an oil bath that had been preheated to a temperature above the melting points of both the bisacid and the tetrakispyridyl. The mixture was stirred for 2 min after all materials had melted and were in the isotropic state unless otherwise noted. The vial was then removed from the oil bath and cooled to room temperature. The network was removed from the flask and subsequently analyzed. The components used to produce these networks are given in Figure 1; a 1 : 1 complex of the tetrapyridyl, **p,** and the diacid, **3,** from that figure would then be referred to as **3/p,** for example.

## PET and its tetrapyridyl complexes

Dimethyl terephthalate (KoSa, 239.6 g), ethylene glycol (Aldrich, 174.7 g), manganese acetate (Aldrich, 0.089 g), and antimony oxide (Riedel de Haen, 0.091 g) were charged to a 0.5-L 316-ss polymerization autoclave equipped with a mechanical stirrer, a distillation column, and a gas adaptor. The reactor heating mantle was set at 220°C, with agitation of approximately 10 rpm. Methanol evolution was observed starting at approximately 160°C; over 120 min, approximately 91 mL of methanol was collected, with a final reaction temperature of 229°C at this point. Once methanol evolution was complete, polyphosphoric acid (0.54 g of a 10% w/w solution in ethylene glycol; Rhodia) was added; the reactor heating mantle was set for 285°C, and vacuum was applied. A final reactor pressure of $<$0.3 Pa was obtained after 120 min. Once the final vacuum was achieved, an additional 55 min were required to obtain the target melt viscosity (as measured by agitator motor current required to maintain 10 rpm). With the completion of the polymerization, vacuum was replaced with approximately 30 psig of nitrogen pressure, and the polymer was extruded through a port on the bottom of the reactor into room temperature water. Intrinsic viscosity was measured

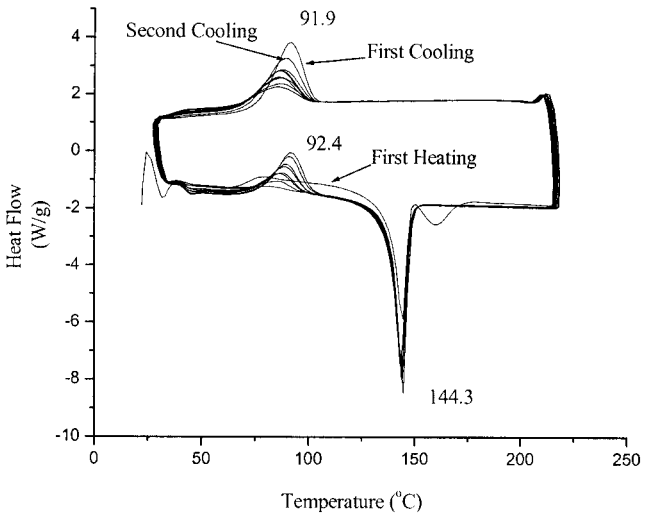


**Figure 2** 4/p network, scans 1–9.

for each polymer sample, using a 1% (w/w) solution of polymer in dichloroacetic acid, using PET viscosity coefficients.

This polymerization experiment was repeated, with the addition of 2.8 g **(1),** 13.0 g **(1),** and 2.8 g **(2)** 15 min prior to extrusion, to give polymers containing 1.2, 5.5, and 1.2 wt % of the tetrapyridyl modifiers, respectively.

### Oxygen transport measurements

Plaques of amorphous polymer were compression molded according to a literature method.[25] Test specimens were cut from the plaques, mounted, and oxygen fluxed at 25°C and 0% relative humidity, and 1 atm pressure was measured with a MOCON OX-TRAN 2/20. The diffusivity ($D$) and permeability ($P$) values for each test were obtained by fitting the flux-time curve to the solution of Fick's second law. The error in determining the two fitting parameters, $P/l$ and $D/l2$, was estimated at less than 2%.[25] Each material was tested in duplicate.

**TABLE I**
**Sum of Crystallization Enthalpies of Cooling Cycle and Subsequent Heat Cycle for 4/p Network**

| (Cool, heat) cycles | Total enthalpy (J/g) |
|---|---|
| (1, 2) | 46.6 |
| (2, 3) | 43.4 |
| (3, 4) | 43.6 |
| (4, 5) | 38.4 |
| (5, 6) | 38.4 |
| (6, 7) | 41.3 |
| (7, 8) | 39.7 |
| (8, 9) | 37.7 |
| (9, 10) | 36.5 |
| (10, 11) | 36.0 |
| (11, 12) | 38.5 |
| (12, 13) | 38.5 |
| (13, 14) | 34.0 |
| (14, 15) | 34.9 |
| (15, 16) | 34.3 |
| (16, 17) | 34.6 |
| (17, 18) | 34.8 |

**TABLE II**
**Sum of Crystallization Enthalpies of Cooling Cycle and Subsequent Heat Cycle for 4/m Network**

| (Cool, heat) cycle | Total enthalpy (J/g) |
|---|---|
| (1, 2) | 25.2 |
| (2, 3) | 19.8 |
| (3, 4) | 19.8 |
| (4, 5) | 18.2 |
| (5, 6) | 19.6 |

## RESULTS AND DISCUSSION

### Supramolecular systems

The materials used in this study are given in Figure 1. The network formed from tetraethylene glycoxy bis-(benzoic acid), **4,** and the *para*-tetrapyridyl netpoint, **p,** was previously reported by Griffin and coworkers[24]; those results are in general agreement with the results reported herein. DSC data for network materials produced from the starting materials of Figure 1 are presented in Figures 2–13. Compiled charts of the crystallization enthalpies observed in the cooling cycle and subsequent heating cycles for the **4/p** and **4/m** systems are given in Tables I and II.

The 3/p and 4/p (Figs. 3–5) networks displayed a modulated decrease in the crystallization events (as observed in the cooling cycle of the DSC) and a subsequent increase in the cold crystallization events in the heating cycle. The modulation was more pronounced in the 3/p networks. The 4/m (Fig. 6) net-

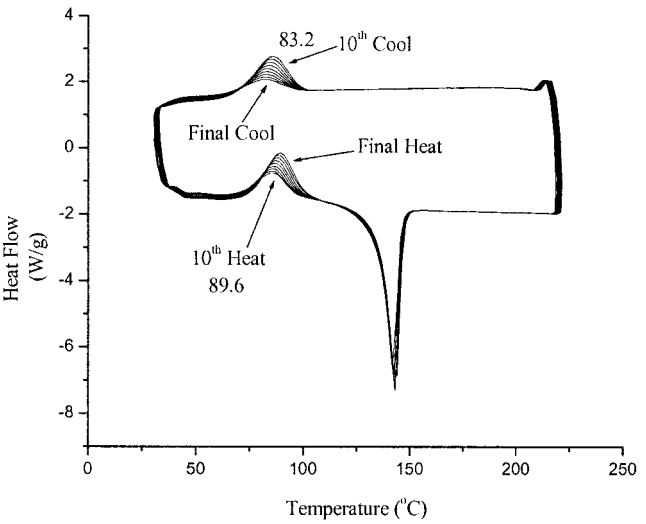


**Figure 3** 4/p network, scans 10–18.

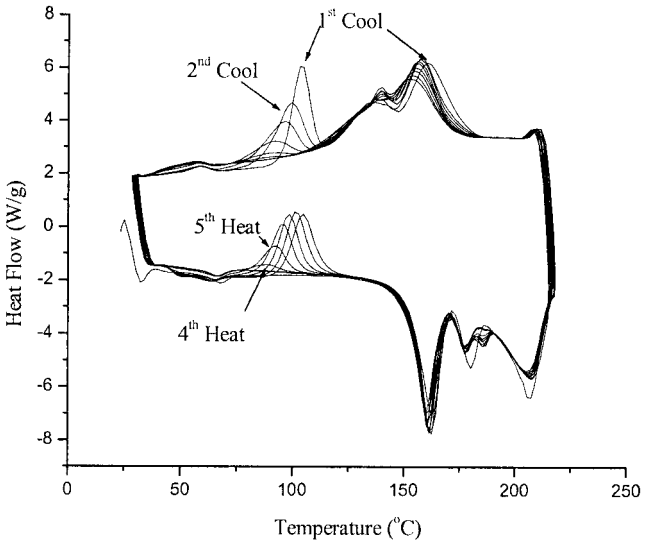


**Figure 4** 3/p network, scans 1–9.

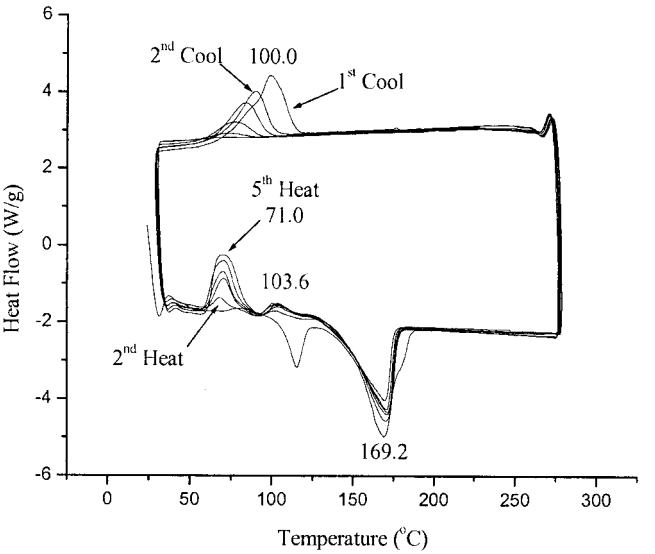


**Figure 6** 4/m network.

work displayed a small amount of the modulation behavior, with the appearance of a second cold crystallization event in later heat/cool cycles. The 4s/p (Fig. 7), 5/p (Fig. 8), and 4,4s/p (Fig. 10) networks displayed no crystallization effects in either the cooling or the heating cycles. Finally, the 5/m network displayed very small crystallization events in the cooling and heating cycles of the DSC thermograms. 4/p network materials treated in the isotropic melt for extended periods of time—1 h (Fig. 11), 3 h (Fig. 12), and 21 h (Fig. 13)—displayed thermal behavior consistent with that of a network treated with multiple heat/cool cycles.

These networks displayed unusual thermal behaviors based on their previous exposure to an isotropic melt. This unusual behavior was observed as an incremental hysteresis (suggestive of memory) observed during repetitive DSC cycle cooling curves. That is, a given crystallization transition was of lower temperature and enthalpy than the previous transition, but of higher temperature and enthalpy than the next transition.

A comparable increase was observed in the cold crystallizations in the heating cycle. We attribute the shifting nature of these transitions to the reversibility of the hydrogen bond. These networks were capable of being severed at the network-forming hydrogen-bond associations and melted into discrete small molecules. As the sample cooled, the hydrogen bonds reformed and a new network was formed with a slightly different morphology than the parent network. Each subsequent thermal treatment (heating into the isotropic/cooling to the solid) altered the

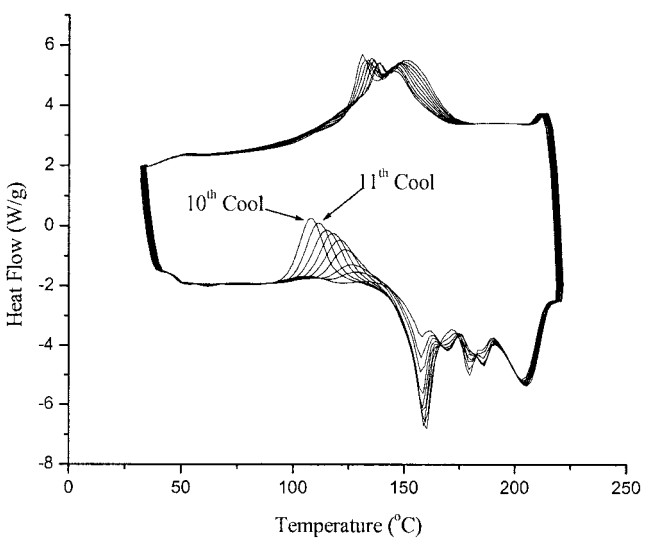


**Figure 5** 3/p network, scans 10–18.

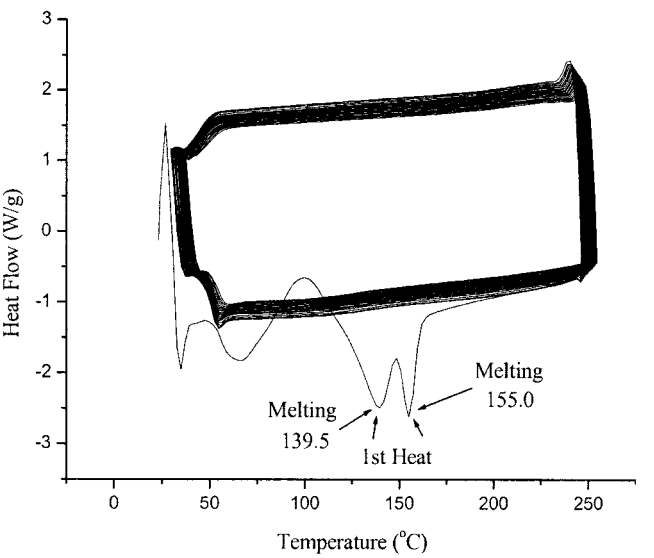


**Figure 7** 4s/p network.

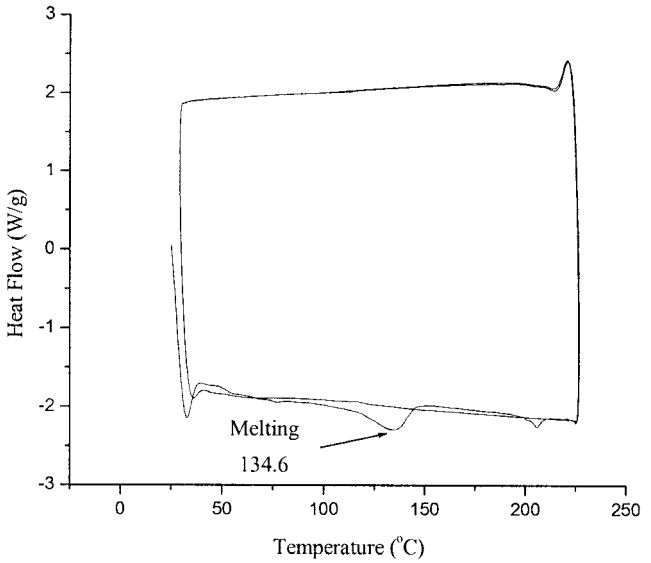


**Figure 8** 5/p network.

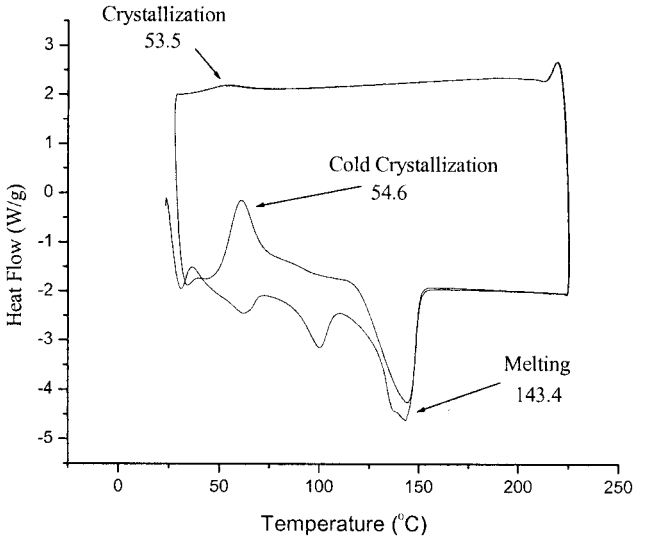


**Figure 10** (4/4s)/p network.

macrostructure of the network slightly. Incremental changes in observed DSC melting behaviors, as a result of melting and recystallization, is a well-known phenomenon that explains both double-melting peaks in polyesters,[26] and the time/temperature-dependent thermal behavior of liquid crystalline polymers.[27] It should be noted (as seen in Tables I and II) that from one thermal cycle to another, there was little decrease in the sum of the enthalpies of the crystallization and cold crystallization transitions, whereas on a global scale, the overall enthalpy decreased slightly. These materials were subjected to the same analysis after several months of treatment at room temperature. The results are identical to those obtained within 1 day of the network (and hydrogen bond) formation. This would indicate that the molecular mobility at room temperature is not sufficient to allow for large-scale chain reorganization.

In an attempt to study the effects of extended time periods in the isotropic melt on the morphological characteristics of the networks, a sample of the tetraethyleneglycoxy bis-4-benzoic acid (4) in complex with the para tetrapyridyl (p) was stirred under argon in the melt state for 1, 2, 3, 4, and 21 h. These timed samples were then thermally analyzed. The thermogram of the 1-h sample resembled a thermogram for the same network composition that had been analyzed for several heat/cool cycles (decreasing crystallization enthalpies and increasing cold crystallization enthalpies with very little change in the melting transition of the network). The analyses of the 2, 3, and 4-h samples

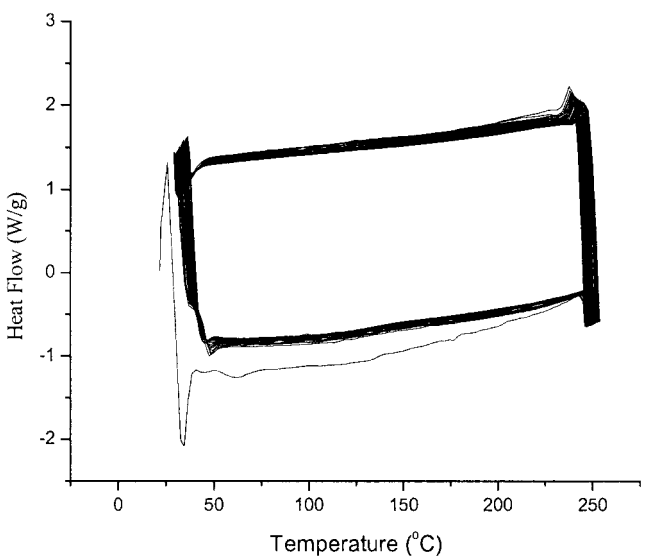


**Figure 9** 5/m network.

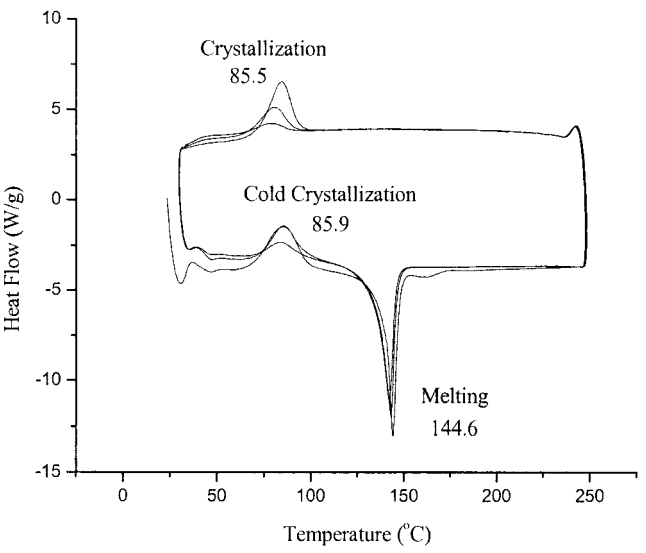


**Figure 11** 4/p network 1 h in the melt.

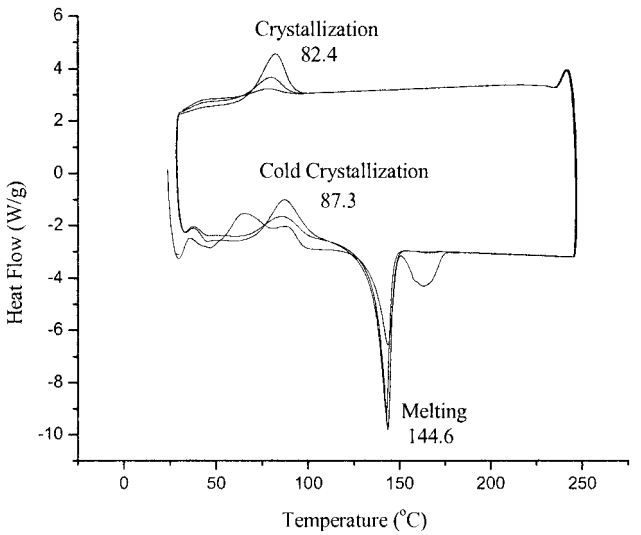


**Figure 12** 4/p network 3 h in the melt.

were also similar to the extensively analyzed complexes. The sample maintained in the isotropic state for 21 h had no crystallization observable in the cooling cycle and also possessed a broad cold crystallization event immediately prior to the melting transition. It appears that most of the crystallinity had been lost from the sample.

The overall shifts in crystallization temperatures and crystallization enthalpies as observed in both cooling and heating cycles are consistent with the concept of perfect networks, as postulated by Meijer and coworkers.[23] This concept states that structures formed by their networks have greater physical integrity because the hydrogen bonds impart reorganization of the chain structures as compared to the covalent analog. The lability of the hydrogen bond, particularly in the single- association case, would allow for macroscopic rearrangements of the chain structure that would not be possible in the covalent network. The supramolecular networks can reorganize, forming a new and possibly more stable chain structure with the input of sufficient thermal or mechanical energy. Such a concept governing supramolecular structures is similar to emerging theoretical models describing the folding of proteins, which rely on the fundamental concept that a memory effect governs the conformation of biopoplymers existing within local energy minima.[28] The ideal structure for these single association networks would appear to be noncrystalline in morphology, as the crystallinity in the samples dissipates after multiple thermal treatments.

The shorter spacers within the acid complex produce more crystallinity in the sample (Figs. 4 and 5). The presence of this complex crystallinity in the sample would seem to indicate that the shorter chain may not achieve the ideal structure through thermal treatments as quickly as do longer chains, which have more conformational mobility and a greater flexibility. The netpoints in the shorter chain networks are considerably closer together than in the longer chain complexes, and, therefore, would require more rearrangement to achieve an ideal structure. When the pentaethylene glycoxy acid species is used, very little crystallinity is observed, and any that is seen is quickly destroyed through thermal treatments, as seen in Figures 8 and 9. A lower degree of cold crystallization is observed in these systems—this would seem to be counterintuitive, as the longer spacers would provide for more flexibility in the network and allow for more conformational mobility and better packing and crystal structure. It is possible that the longer chains have sufficient length that the ideal structure is obtained more quickly than with the shorter acids. When the methoxy-substituted acid was used as a hydrogen-bond donor (4s/p), there was very little crystallinity observed in the first heating and cooling of the sample (Fig. 10). The small amount of crystallinity that existed was quickly lost from the sample in the next thermal cycling. The methoxy-substituted acid may not be able to pack efficiently because of steric restrictions in the side-by-side molecular packing.

Conceivably, the network should rearrange to an ideal configuration immediately after going into the isotropic melt, as the chains are free to flow past one another. The fact that it takes some of these complexes 18 or more cycles to find an optimum conformation is quite surprising. Combined with the observation that the network did not return to the premelt state, it would seem that the supramolecular network displayed a type of memory structure: the material would change slowly over time and form new structures from the template provided by the previous morphology. As the complex was subjected to more and more thermal cycles, the morphology of the sample would shift toward a more noncrystalline struc-

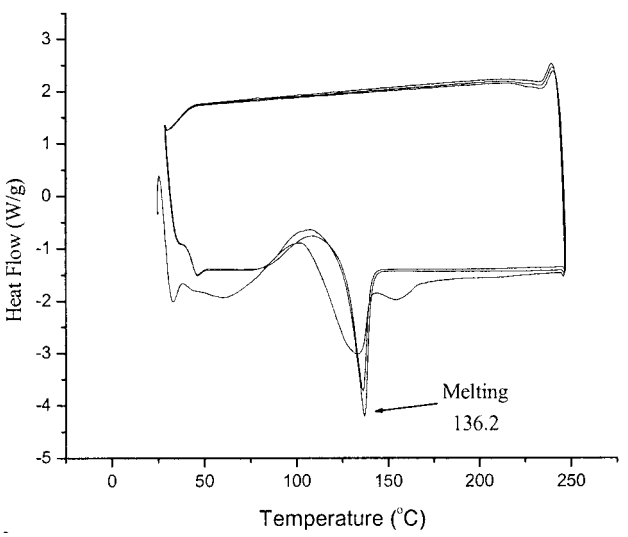


**Figure 13** 4/p network 21 h in the melt.

**TABLE III**
**Pyridgl-Modified PET Polymer Samples**

| Additive | Additive level (wt %) | Physical description | IV | $T_g$ (°C) | $T_m$ (°C) |
|---|---|---|---|---|---|
| None | — | Off-white solid | 0.61 | 81.3 | 258.6 |
| (**1**) | 1.2 | Yellow solid | 0.58 | 78.1 | 256.4 |
| (**1**) | 5.50 | Yellow solid | 0.59 | 71.1 | 252.7 |
| (**2**) | 1.2 | Decomposed black solid | — | — | — |

ture. It should be noted, however, that the crystallization seemed to be regained in the subsequent cold crystallization transitions observed by DSC. Enthalpic comparisons found that for the 4/p and 4/m networks, the sum of the crystallization observed in a cooling cycle and the cold crystallization in the subsequent heat were similar across many heat/cool cycles. As there was a gradual decrease in the enthalpic sum of the transitions, it would appear that the crystallization was reduced over time. A lower rate was observed for the 3/p species. Additionally, the enthalpic sums mentioned above were also nearly equal to the enthalpy of the melting transition observed in the same heat cycle as the cold crystallization event. This information would seem to indicate that there is a net crystallinity in the sample that is met throughout the heating of the sample, but would appear to be slowly removed from the material.

Measurements of the effects of temperature and time on the morphology of the *meta*-networks were also carried out. The *meta*-tetrapyridyl networks had less crystallinity and less crystalline complexity that the *para*-networks. This is believed to be caused by the nonlinear association induced by the *meta*-netpoint. The hydrogen bond forms approximately perpendicular to the symmetry plane of the netpoint. This would produce an awkward geometric network structure especially compared to the *para*-species, in which the association extends the plane of the molecule out further through the hydrogen bond.

## Modified polymer systems

PET polymer samples containing 0, 1.2, and 5.50 mol % of **(1)** were produced and characterized (see Table III). Attempts to produce PET modified by **(2)** led to the production of a black, char-like material that showed no physical integrity and were therefore discarded. The PET sample containing 5.5% of **(1)** appeared to contain some heterogeneous particles, and therefore, was not further tested as well. The thermal behaviors of PET and the 1.2% tetrapyridyl-modified polymer system were examined by DSC (Figs. 14–15); unlike unmodified PET, the PET/**(1)** system showed a thermal history-dependent behavior. It is interesting to note that the phase transitions in the modified PET sample occur at slightly lower temperatures than those of the unmodified PET, perhaps indicating a destabilization of the phases with the presence of a reversible, hydrogen-bonded netpoint. The formation of single hydrogen-bond networks on a molecular scale is proposed through the pyridyl nitrogen **(1)** (the netpoint) and the acid end groups of PET chains (acid end groups typically constitute 25–35% of total end-group concentration). This proposed network is similar in structure to other networks suggested to arise from the interaction of tetrafunctional pyridyls and monomeric diacids.[8,9] The PET/netpoint samples of this study would be expected to possess a much greater chain length and a lower acid end-group concentration, given the differences between linear dicarboxylic acid and high molecular weight polyesters. Unlike polyesters containing similar levels of covalent crosslinks, the hydrogen-bonded networks of this study are thermoplastic and melt processible.

Analysis of the cold crystallization and crystallization events in the sample containing **(1)** indicated a modulated transition series. The magnitude of ther-

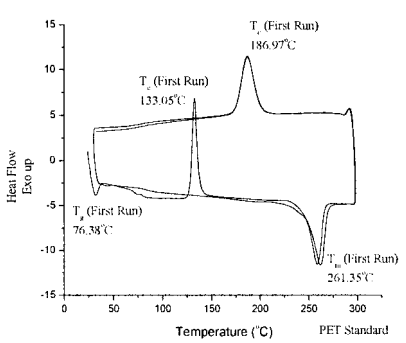


**Figure 14** DSC thermal cycling of PET.

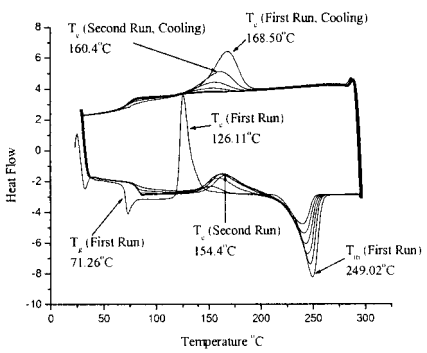


**Figure 15** DSC thermal cycling of tetrapyridyl-modified PET.

mal transitions in the DSC experiment decreased with repeated scans. The cold crystallization temperature increased with sequential thermal cycles, whereas the crystallization transitions from the melt decreased in temperature as multiple scans ensued. These results are similar to those obtained with the small molecular/supramolecular network systems described above. As with the above small molecule systems, the overall shifts in crystallization temperatures and crystallization enthalpies as observed in both cooling and heating cycles for the modified PET systems can be explained by the perfect network theory. That the amorphous structures generated in DSC experiments were not already established in the polymer as extruded from the polymerization reactor (wherein significant time/temperature are encountered) also suggests that with sufficient heat history, the hydrogen-bonding network can be thoroughly disrupted.

Given the postulated changes in polymer structure deduced from the thermal behavior of PET/**(1)** complexes, changes in physical properties could be anticipated when PET is modified by the addition of hydrogen-bonding netpoints. Oxygen transport properties were chosen as a probe for such property modifications, because this property depends heavily upon the nature of the glassy state and is of specific interest in many commercial applications of PET. Samples of PET and of PET/**(1)** containing 1.2% tetrapyridyl were compression molded into 7-mil, amorphous plaques, which were then tested. Oxygen permeation data for the pair of materials are given in Table IV, which shows a nearly twofold reduction in oxygen permeation rate resulting from addition of **(1)** to the polymer. Further analysis of the transport data reveals that this significant reduction in oxygen permeation is entirely the result of decreased diffusivity of oxygen through the polymer (solubility of oxygen in polymer actually increased slightly as a result of tetrapyridyl addition).

It has been well established that solubility of oxygen in PET-based systems can be explained as resulting from static-free volume, which is proportional to the difference between polymer glass transition temperature ($T_g$) and the temperature at which the measurements are made.[13,14] Given that the PET/(1) composition tested shows a slightly lower $T_g$ value than unmodified PET, it is surprising that its oxygen solubility coefficient is significantly higher than that of the base polymer. The implication is that hydrogen-bonding interactions modify the nature of static-free volume. Increasing the amount of static-free volume appears unlikely in view of the higher density of PET/**(1)** compared to PET. Possible reasons for the unexpectedly high solubility include changes in the distribution of free volume that would increase accessibility to oxygen and/or changes in the state of sorbed oxygen that would increase its density.

Oxygen diffusivity through PET systems has similarly been demonstrated to result from dynamic-free volume, which correlates with segmental motions that are measured as the sub-$T_g$ relaxation intensity.[14] This modification of dynamic-free volume by incorporation of hydrogen-bonding interactions is fundamentally different than what is observed when covalent crosslinks are incorporated in PET. Incorporation of the trifunctional monomer trimesic acid into a PET/isophthalaic acid copolymer resulted in increased permeation and diffusivity coefficients versus the noncrosslinked polymer (solubility coefficient conformed with the general relationship between solubility and $T_g$).[29] A fundamental difference, therefore, appears to exist between how hydrogen-bonding netpoints and covalent crosslinks modify the glassy state of PET, and therefore, its gas transport properties.

## CONCLUSIONS

Highly crosslinked networks were produced through a series of diacids and tetrakis pyridyls. These materials displayed a shift in the crystallization behavior over multiple heat/cool cycles. In many of these cases, the observed pattern demonstrated a diminished level of crystallinity in the cooling cycle of the thermogram, with increased cold crystallinity in the subsequent heating cycle. Further analysis showed that networks made from shorter chained acids (the hydrogen-bond donor) displayed more complex crystallization behavior in the thermograms, and longer acids gave rise to very little crystallinity in the networks. By using a substituted acid as the proton donor produced a noncrystalline material as well, as did mixtures of tetrakis pyridyl netpoints. Analyses of the complexes treated for extended periods in the melt were undertaken in an effort to determine the origin of the crystalline shifting. It was found that materials exposed to the isotropic melt for extended periods mimicked the phase behavior of samples thermally treated through multiple cycles of comparable length.

The shifting of these patterns seems to indicate that the material was moving toward a thermodynamically ideal structure. This structure would seem to be non crystalline in nature. The fact that some of the networks required such a long thermal treatment was surprising. Even considering the potential for reconfiguration of the associative network structure, it would seem that the network would be able to find the favored state at a greater rate. These materials display a type of memory in which the networks seem to remember the morphological structure previous to the melt and improve upon that structure in the next cooling cycle. Covalent networks lack the ability to rearrange and form a more thermodynamically favored structure, due to the relative permanence of the covalent bond.

**TABLE IV**
**Barrier Properties of Polyesters**

| Sample | Density (g $cm^{-3}$) | Permeability | Diffusivity | Solubility |
|---|---|---|---|---|
| PET | 1.3350 ± 0.0006 | 0.469 ± 0.002 | 5.6 ± 0.2 | 0.098 ± 0.002 |
| PET/1.2%(I) | 1.3452 ± 0.0005 | 0.251 ± 0.001 | 2.4 ± 0.1 | 0.121 ± 0.001 |
| PET/15%I[a] | 1.3390 ± 0.0025 | 0.324 ± 0.01 | 4.2 ± 0.1 | 0.090 ± 0.003 |
| PET/15%I/1.2%T[b] | 1.3412 ± 0.0008 | 0.347 ± 0.001 | 4.8 ± 0.1 | 0.084 ± 0.001 |

[a] Isophthalic acid.
[b] Trimesic acid. Permeability in [mL(STP) cm $m^{-2}$ $atm^{-1}$ $day^{-1}$]. Diffusivity in ($\times 10^{-13}$ $m^2$ $s^{-1}$). Solubility in [mL(STP) $cm^{-3}$ $atm^{-1}$].

The acids with shorter chains display a more complex crystallization pattern because the chains lack sufficient flexibility to acquire that ideal structure quickly. Longer chain acids find that structure with greater ease, consistent with their higher molecular mobilities. Analyses of both the mixed-netpoint and the substituted acid complexes give credence to the concept of crystallinity being derived from the acid species. The exposure of the networks to sufficient heat energy to force them into the isotropic melt for long periods of time produced networks of similar morphology to the samples treated with multiple thermal cycles. This adds further credence to the concept that the time spent in the isotropic melt gives rise to the shifting of the crystallization behavior.

The network/memory phenomena observed in small-molecule diacid/tetrapyridyl systems also appeared to exist when PET polymer was used as the source of carboxylic acid functionalities. The same time-dependent behaviors, suggestive of sequential steps toward thermodynamically optimum states, was observed when the PET/tetrapyridyl systems were thermally cycled. It was also observed that complexation of tetrapyridyl with PET brought about a significant change in oxygen gas-barrier properties; these changes were opposite to those obtained when covalent crosslinks were introduced into PET.

Financial support from KoSa and from NSF-EPSCoR are greatly appreciated. Dr. Anna Polyakova and Professor Anne Hiltner of Case Western Reserve University provided the oxygen transport measurements, which are gratefully acknowledged.

## References

1. Gong, B. Synlett 2001, 5, 582.
2. Fenniri, H., Mathivanan, P, Vidale, K. L., Sherman, D. M., Hallenga, K., Wood, K. V., Stowell, J. G. J Am Chem Soc 2001, 123, 3854.
3. Rudkevich, D. M. Chem Eur J, 2000, 6 (15), 2679.
4. Balzani, V., Credi, A., Raymo, F. M., Stoddart, J. F. Angew Chem Int Ed 2000, 39, 3348.
5. Kato, T. Supramol Sci 1996, 3, 53.
6. Vogtle, F. Supramolecular Chemistry; Wiley: West Sussex, 1991.
7. Bladon, P.; Griffin, A. Macromolecules 1993, 26, 6604.
8. Lehn, J.; Mascal, M.; DeCain, A.; Fischer, J. J Chem Soc Chem Commun 479, 1990.
9. Lehn, J.; Mascal, M.; DeCian, A.; Fischer, J. J Chem Soc: Perkin Trans 1992, 2, 461.
10. Etter, M.; Adsmond, D. J Chem Soc Chem Commun 1990, 589.
11. Etter, M. Acc Chem Res 1990, 120.
12. Periso, F.; Wuest, J. J Org Chem 1993, 58, 95.
13. Wang, X.; Simard, M.; Wuest, J. J Am Chem Soc 1994, 116, 12119.
14. Boucher, E. Simard, M.; Wuest, J. J Org Chem 1995, 60, 1408.
15. Hilger, C.; Stadler, R.; Polymer 1991, 17, 3244.
16. Hilger, C. Stadler, R. Macromolecules 1992, 66, 70.
17. Hilger, C., Stadler, R., Makromol Chem 1991, 192, 805.
18. Seidel, U.; Stadler, R.; Fuller, G. Macromolecules 1994, 2720, 66.
19. Hilger, C. Stadler, R. Macromolecules 1990, 23, 2097.
20. Hilger, C. Drager, M. Stadler, R. Macromolecules 1992, 25, 2498.
21. Lillya, C.; Baker, R.; Huttes, W. Lin, Y. Shi, J. Dickinson, L. Chen, C. Macromolecules 1992, 25, 2076.
22. Sijbesma, R.; Beijer, F.; Brunsveld, L.; Folmer, B.; Hirschberg, K.; Lange, R.; Lowe, J.; Meijer, E. Science 1997, 278, 1601.
23. Lange, R.; Van Gurp, M.; Meijer, E. J Polym Sci, Part A: Polym Chem 1999, 37, 3657.
24. St. Pourcain, C.; Griffin, A. Macromolecules 1995, 28, 4116.
25. Sekelik, D. J.; Stepanov, E. V.; Nazarenko, S.; Schiraldi, D. A.; Hiltner, A.; Baer, A.; J Polym Sci, Part B: Polym Phys 1999, 37 (8), 847–857.
26. Lu, X. F.; Hay, J. N. Polymer 2001, 42, 9423–9431.
27. Hu, X.; Zhou, X. Y.; Yue, C. Y.; Kyotani, M.; Nakayama, K. Macromol Chem Phys 2001, 202, 1743–1749.
28. Locker, C. R.; Hernandez, R. Proc Nat Acad Sci. July 31, 2001, 98 (16), 9074–9.
29. Polyakova, A. Ph.D. dissertation, Case Western Reserve University, 2000.